Available online at www.sciencedirect.com
SCIENCE DIRECT®
Bioorganic & Medicinal Chemistry Letters 15 (2005) 983–987
Bioorganic & Medicinal Chemistry Letters

Identification of nonpeptidic small-molecule inhibitors of interleukin-2

Nathan D. Waal,* Wenjin Yang, Johan D. Oslob, Michelle R. Arkin, Jennifer Hyde, Wanli Lu, Robert S. McDowell, Chul H. Yu and Brian C. Raimundo

Sunesis Pharmaceuticals, Inc., 341 Oyster Point Boulevard, South San Francisco, CA 94080, USA

Received 28 September 2004; revised 18 November 2004; accepted 15 December 2004
Available online 18 January 2005

Abstract—The identification, design, and synthesis of a series of novel sulfamide- and urea-based small-molecule antagonists of the protein–protein interaction IL-2/IL-2Rα are described. Installation of a furan carboxylic acid fragment onto a low-micromolar sulfamide resulted in a 23-fold improvement in activity, providing a sub-micromolar, nonpeptidic IL-2 inhibitor (IC_{50} = 0.60 μM).

Binding of the cytokine interleukin-2 (IL-2) to its receptor (IL-2R) leads to the proliferation of activated T-lymphocytes and stimulation of the T-helper 1 (Th1) immune response.[1–4] Irregular Th1 immune responses play a central role in the development of autoimmune disorders such as rheumatoid arthritis, multiple sclerosis, psoriasis, and graft rejection.[5,6] Two currently marketed antibodies that specifically target the alpha subunit of the IL-2 receptor (IL-2Rα) are known to decrease the incidence of graft rejection;[7,8] however, these agents lack oral bioavailability and induce side effects such as hypersensitivity.[9] A small-molecule inhibitor of the protein–protein interaction IL-2/IL-2Rα could potentially circumvent the disadvantages associated with these immunosuppressive therapies.

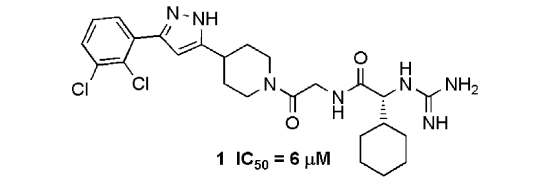

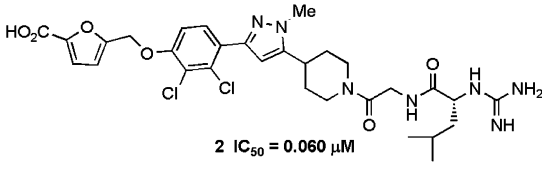

A previous report describes a compound (**1**, IC_{50} = 6 μM) that binds to IL-2, preventing its association with IL-2Rα.[10] Two components critical for the activity of **1**—the polar guanidine and the hydrophobic tricyclic ring system—were initially connected via a dipeptide chain. Optimization of **1** included the installation of a furanoic acid fragment onto the dichlorophenyl ring. This fragment, discovered through Tethering, offered a 30-fold improvement in activity and led to the discovery of a potent inhibitor (**2**, IC_{50} = 0.060 μM).[11] Although the dipeptide provided a useful framework for rapid analog synthesis and SAR development, its potential in vivo liabilities sparked an effort to identify alternate linkages. The co-crystal structures[12,13] of **1** and **3** (a known small-molecule IL-2 inhibitor; IC_{50} = 3 μM)[14] bound to IL-2 offered some guidance into the design of new linkers. The guanidine moiety of **3** forms two hydrogen bonds with a neighboring glutamic acid E62 (Fig. 1). In contrast, the guanidine moiety of **1** forms only one hydrogen bond with E62, and appears to adopt a high-energy conformation relative to **3**. The piperidine ring of **3** complements the protein surface better than the dipeptide, while the cyclohexyl group of **1** occupies a shallow, hydrophobic pocket not accessed by **3** (Fig. 2). We reasoned that the ideal nonpeptidic linker would combine the advantages of **1** and **3**. It was thought that alkyl substituted sulfamide or urea linkers could satisfy the above requirements

Keywords: Fragment assembly; Cytokine; Protein–protein interaction; IL-2.
* Corresponding author. Tel.: +1 650 266 3654; fax: +1 650 266 3501; e-mail: nwaal@sunesis.com

0960-894X/$ - see front matter © 2005 Elsevier Ltd. All rights reserved.
doi:10.1016/j.bmcl.2004.12.045

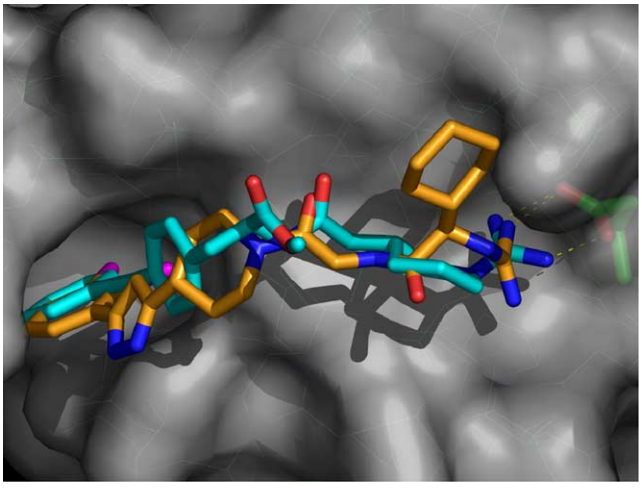

Figure 1. Crystal structures of **1** (orange) and **3** (cyan) bound to IL-2. Glutamic acid (E62) is shown in green.[15]

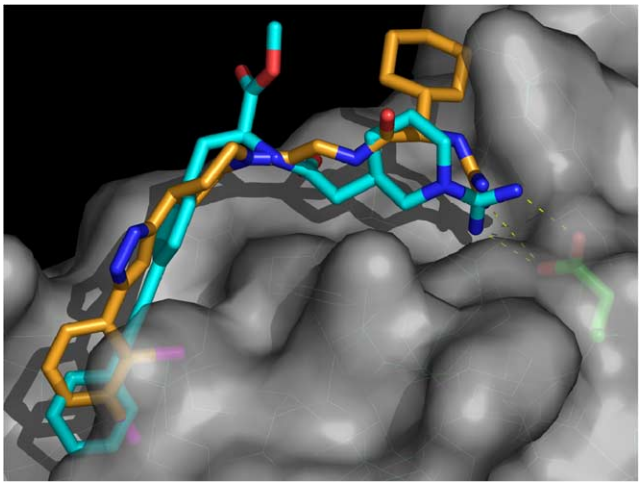

Figure 2. Crystal structures of **1** (orange) and **3** (cyan) bound to IL-2. The piperidinyl ring of **3** better complements the protein surface than the dipeptide of **1**. The cyclohexyl group of **1** sits in a shallow hydrophobic pocket not accessed by **3**.

and be accessed quickly from readily obtainable diamine precursors.

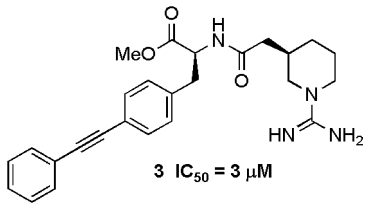

Sulfamides and ureas were synthesized in five steps from intermediate **4** (Scheme 1).[16] The requisite sulfamoyl and carbamoyl chlorides (**5**, **6**) were obtained by treating **4** with sulfuryl chloride or triphosgene, respectively. In generating **5**, slow addition of sulfuryl chloride at reduced temperature was necessary to suppress chlorination at the 4-position of the pyrazole ring. Intermediates

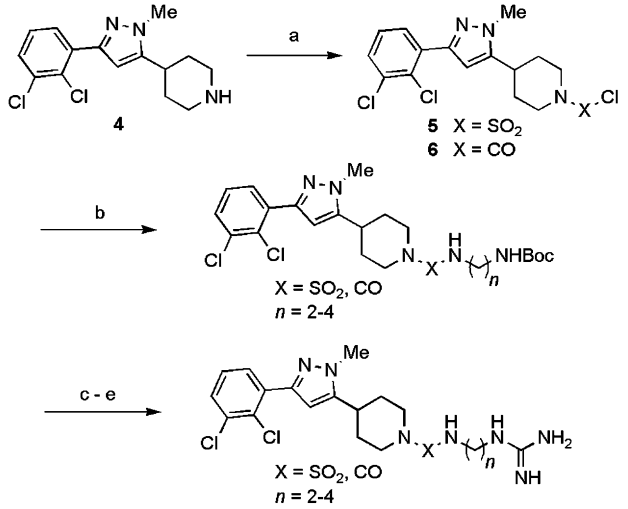

Scheme 1. Reaction conditions: (a) SO_2Cl_2 or triphosgene, Et_3N, CH_2Cl_2, −78 °C → rt, 70–80%; (b) mono-Boc-protected diamine, Et_3N, CH_2Cl_2; (c) TFA, CH_2Cl_2; (d) *N*,*N*′-bis-Boc-1-guanylpyrazole, Et_3N, MeOH; (e) TFA, CH_2Cl_2, 23–40% after four steps.

5 and **6** were reacted with various mono-Boc-protected diamines[17] to produce sulfamides and ureas, which were subjected to a rapid three-step deprotection, guanidinylation, deprotection sequence. Target compounds were purified via reverse-phase preparatory HPLC.

In order to determine the preferred atom count between the piperidine and guanidine moieties, we synthesized a small set of analogs incorporating alkyl diamine linkers of varying chain lengths. As shown in Table 1, analogs bearing a propanediamine linkage (**9**, **10**) are more active than their ethyl and butyl counterparts (**7**, **8**, **11**, **12**). This finding is consistent with the atom count required for activity of the peptidic parent compounds. In addition, corresponding sulfamides and ureas display similar SAR and are essentially equipotent. Once the appropriate chain length was established we focused our attention on linker substitutions, anticipating that substituents placed on either the internal guanidine nitrogen or the adjacent carbon atom would access the hydrophobic pocket. Results of linker *N*-alkylation are shown in Table 2. Methylation of the internal guanidine

Table 1. Sulfamide and urea linker length dependence

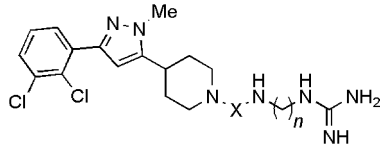

Compds	X	*n*	IC_{50} (μM)[a]
7	CO	2	>100
8	SO_2	2	>100
9	CO	3	29
10	SO_2	3	23
11	CO	4	>100
12	SO_2	4	>100

[a] All reported results were obtained using either a Scintillation Proximity Assay or ELISA.[16]

Table 2. Linker SAR: *N*-alkylation

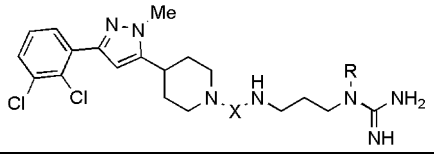

Compds	X	R	IC_{50} (μM)
9	CO	H	29
10	SO_2	H	23
13	CO	Me	16
14	SO_2	Me	14
15	CO	Pr	>100
16	SO_2	Pr	32
17	CO	*i*-Pr	>100
18	SO_2	*i*-Pr	48

nitrogen (**13**, **14**) leads to a slight improvement in activity compared with unsubstituted derivatives **9** and **10**. Compounds **15**–**18** demonstrate that guanidine alkyl substituents larger than a methyl group are generally not favored, although this trend is less pronounced with sulfamides (**16**, **18**). Additional substitutions were made on the carbon atom adjacent to the guanidine (Table 3). Corresponding sulfamides and ureas are generally equipotent. Increasing the alkyl group size has little effect on activity (**19**–**24**), and the presence of isobutyl groups (**23**, **24**) results in compounds that are roughly equipotent to the unsubstituted derivatives **9** and **10**. Furthermore, compounds **25** and **26** confirm a strict dependence on

Table 3. Linker SAR: *C*-alkylation

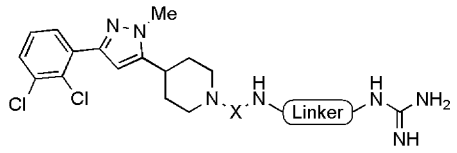

Compds	X	Linker	IC_{50} (μM)
9	CO	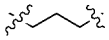	29
10	SO_2	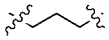	23
19	CO	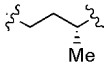	57
20	SO_2	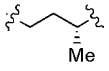	90
21	CO	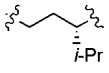	55
22	SO_2	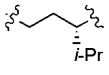	76
23	CO	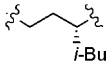	23
24	SO_2	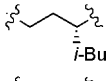	30
25	CO	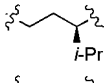	>100
26	SO_2	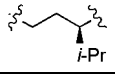	>100

Table 4. Representative diaminobutyric acid derivatives

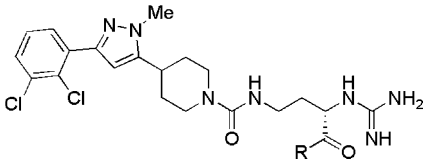

Compds	R	IC_{50} (μM)
27	OH	>100
28	OMe	>100
29		>100
30		7
31		11
32		20
33	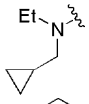	60
34	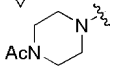	60
35	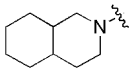	>100

the stereochemistry of linker substituents for activity. The alkyl groups of **25** and **26** are predicted to point into the protein surface, likely causing the lack of activity observed for these compounds. Although no increase in activity is observed relative to **9** and **10**, the tolerance of bulky groups and the stereochemical preference in this region of the protein is consistent with the dipeptide SAR. A diaminobutyric acid-derived linker provided a functional handle for further exploration of the hydrophobic pocket (Table 4). Because corresponding sulfamides and ureas are equipotent and display similar SAR trends, we pursued only one series. Polar substituents lead to inactive compounds (**27**–**29**), while more lipophilic groups result in increased activity (**30**–**32**). Activity diminishes, however, as amide substituents become larger (**33**–**35**). With **30**, the goal of replacing the peptidic linker while retaining potency relative to **1** was achieved.

Finally we wanted to confirm that addition of the furanoic acid fragment to this new series would result in a similar boost in affinity as observed with **2**. Sulfamide **14** was chosen as a low-micromolar starting point. Scheme 2 outlines the synthetic route employed, starting from intermediates **36** and **38**.[16] Alkyne **36** was treated with hydrochloric acid, followed by sulfuryl chloride and the appropriate Boc-protected diamine to provide **37**. Acid chloride **38** was reacted with **37** under palladium-mediated conditions to give an alkynyl ketone, which was cyclized with methylhydrazine to provide pyrazole **39** as one regioisomer. Removal of the silyl protecting group with tetrabutylammonium fluoride

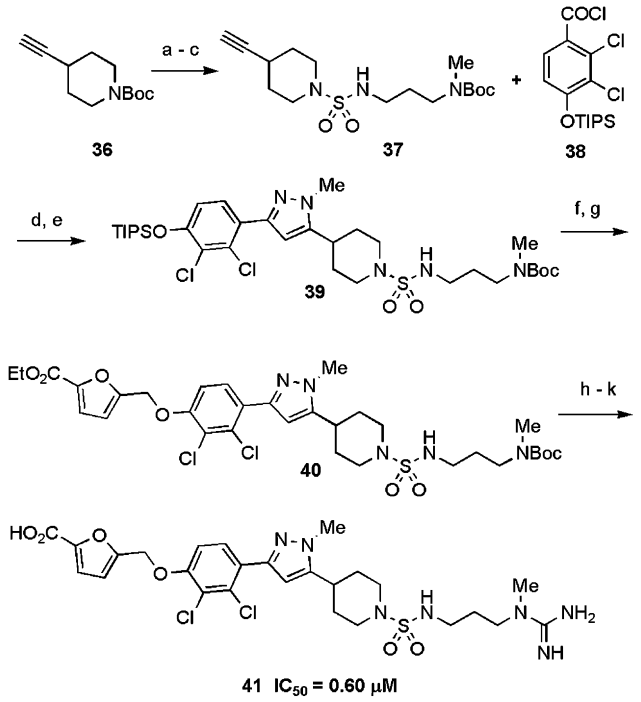

Scheme 2. Reaction conditions: (a) 4 N HCl/dioxane, quant.; (b) SO_2Cl_2, Et_3N, CH_2Cl_2; (c) *N*-Boc-*N*-methyl-1,3-diaminopropane, Et_3N, CH_2Cl_2, 27% after two steps; (d) CuI, $Pd(PPh_3)_2Cl_2$, Et_3N, toluene; (e) H_2NNHMe, EtOH, 30% after two steps; (f) TBAF, THF, 0 °C; (g) ethyl 5-chloromethyl-2-furancarboxylate, K_2CO_3, DMF, 55 °C, 22% after two steps; (h) LiOH, THF/H_2O, quant.; (i) TFA, CH_2Cl_2; (j) *N*,*N*′-bis-Boc-1-guanylpyrazole, Et_3N, MeOH; (k) TFA, CH_2Cl_2, 25% after three steps.

gave the phenol, which was alkylated using potassium carbonate and ethyl 5-chloromethyl-2-furan carboxylate to afford **40**. Saponification of **40** followed by the three-step guanidinylation sequence mentioned above supplied **41**. Addition of the furanoic acid to **14** imparts a 23-fold improvement in activity, resulting in an IC_{50} of 0.60 μM. A computational model of **41** with IL-2 (Fig. 3) indicates a binding mode in the adaptive region similar to that observed for **2**. Furthermore, the model suggests that the sulfamide linkage facilitates the desired bidentate interaction between the guanidine moiety and E62.

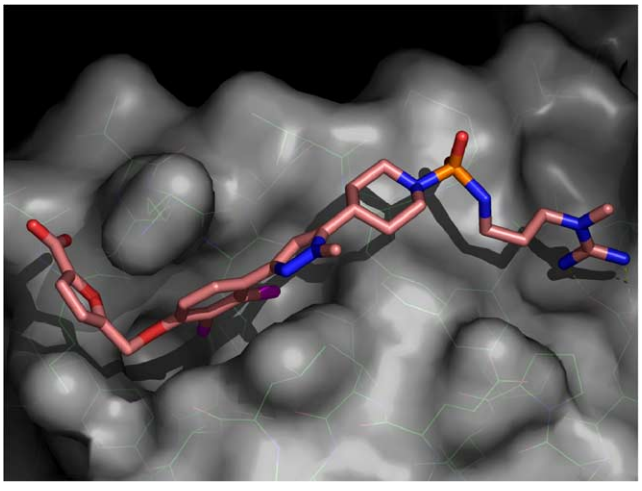

Figure 3. Computational model of **41** with IL-2.

In conclusion, we have identified a nonpeptidic series of inhibitors of the protein–protein interaction IL-2/IL-2Rα. The structure–activity relationship was developed through the evaluation of a variety of linker substituents, which yielded several low-micromolar hits. Merging a low-micromolar sulfamide with a binding element identified through Tethering resulted in the discovery of a sub-micromolar inhibitor. Further investigation of this series is currently in progress.

Acknowledgements

The authors wish to thank Stuart Lam, Charles Hatchette, Tom Webb, and Alex Hsi for their support with RP-HPLC purifications.

References and notes

1. Rubin, L. A.; Nelson, D. L. *Ann. Intern. Med.* **1990**, *113*, 619.
2. Nelson, B. H.; Willerford, D. M. *Adv. Immunol.* **1998**, *70*, 1.
3. Waldmann, T. A.; Dubois, S.; Tagaya, Y. *Immunity* **2001**, *14*, 105.
4. Nelson, B. H. *Curr. Dir. Autoimmun.* **2002**, *5*, 92.
5. LeMoine, A.; Goldman, M.; Abramowicz, D. *Transplantation* **2002**, *73*, 1373.
6. Singh, V. K.; Mehrotra, S.; Agarwal, S. S. *Immunol. Res.* **1999**, *20*, 147.
7. Berard, J. L.; Velez, R. L.; Freeman, R. B.; Tsunoda, S. M. *Pharmacotherapy* **1999**, *19*, 1127.
8. Waldmann, T. A.; O'Shea, J. *Curr. Opin. Immunol.* **1998**, *10*, 507.
9. For information regarding the side effects of basiliximab and daclizumab, see Letters to Healthcare Providers: http://www.fda.gov/medwatch/SAFETY/2000/simule.htm http://www.fda.gov/medwatch/SAFETY/2003/zenapax.htm.
10. Braisted, A. C.; Oslob, J. D.; Delano, W. L.; Hyde, J.; McDowell, R. S.; Waal, N.; Yu, C.; Arkin, M. R.; Raimundo, B. C. *J. Am. Chem. Soc.* **2003**, *125*, 3714.
11. Tethering is a registered trademark of Sunesis Pharmaceuticals for its fragment-based drug discovery.
12. Thanos, C. D.; Randal, M.; Wells, J. A. *J. Am. Chem. Soc.* **2003**, *125*, 15280 (PDB ID 1PW6).
13. Arkin, M. R.; Randal, M.; Delano, W. L.; Hyde, J.; Luong, T. N.; Oslob, J. D.; Raphael, D. R.; Taylor, L.; Wang, J.; McDowell, R. S.; Wells, J. A.; Braisted, A. C. *Proc. Natl. Acad. Sci. U.S.A.* **2003**, *100*, 1603 (PDB ID 1M48).
14. Tilley, J. W.; Chen, L.; Fry, D. C.; Emerson, S. D.; Powers, G. D.; Biondi, D.; Varnell, T.; Trilles, R.; Guthrie, R.; Mennona, F.; Kaplan, G.; LeMahieu, R. A.; Carson, M.; Hen, R.-J.; Liu, C.-M.; Palermo, R.; Ju, G. *J. Am. Chem. Soc.* **1997**, *119*, 7589.
15. DeLano, W. L. The PyMOL Molecular Graphics System.' DeLano Scientific LLC: San Carlos, CA, USA. http://www.pymol.org.
16. Raimundo, B. C.; Oslob, J. D.; Braisted, A. C.; Hyde, J.; McDowell, R. S.; Randal, M.; Waal, N. D.; Wilkinson, J.; Yu, C. H.; Arkin, M. A. *J. Med. Chem.* **2004**, *47*, 3111.

17. Diamines were prepared according to common literature methods. Typically, *N*-protected amino acids were reduced to amino alcohols, which were mesylated and displaced using NaCN. Reduction of the cyano group provided the desired mono-protected propanediamines.